

# Lecture 10 Interferometric Imaging

## Table of Contents

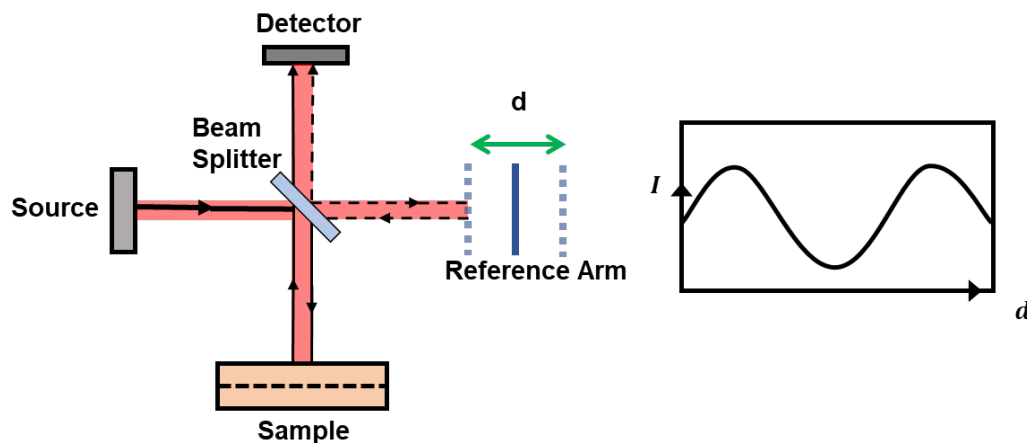
1. Continuous wave interferometry.....	1
1.1 Michelson interferometry setup.....	1
1.2 Interferometry with swept reference arm.....	2
1.2.1 Depth topography.....	4
1.3 Limitations of single wavelength CW interferometry for axial imaging.....	5
2. Interferometry with a swept frequency CW source.....	8
3. Interferometry with low coherent source.....	12
3.1 Interferometry with pulsed wave.....	12
3.2 Time domain Optical Coherent Tomography (OTC).....	16
3.2.1 Comparison of TD- vs. FD-OCT.....	16

## 1. Continuous wave interferometry

### 1.1 Michelson interferometry setup

A coherent monochromatic wave can be used to measure distance and time delay using interferometry. The most common setup is used in a free-space system for imaging purposes is the Michelson Interferometer, shown in ILL 1.1.

The source is illuminated on a beam splitter, which divides the beam into the sample arm (to the object), and the reference arm (to the mirror). The beam is reflected from each path and recombined by the beam splitter on the detector. The interference of the reflected beam from the sample arm and the reference arm is detected on the detector.



ILL. 1.1 Michelson interferometer setup

When a wave travels a distance  $d_o$ ,

it undergoes a phase shift  $\phi = kd_o = 2\pi \frac{d_o}{\lambda}$ , where  $\lambda$  = wavelength.

A time delay  $\tau_o$  is equivalent to a phase shift  $\phi = \omega\tau_o$ , where  $\omega$  = angular frequency.

Since the time delay associated with a distance  $d_o$  is  $\tau_o = \frac{d_o}{c}$ ,

$$\phi = \omega\tau_o = \omega \frac{d_o}{c} = 2\pi \frac{d_o}{\lambda}$$

By measuring the phase, the distance and time delay can be estimated.

The phase shift may be measured by the use of an interferometer.

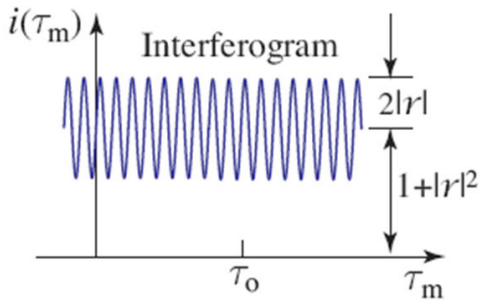
## 1.2 Interferometry with swept reference arm

The intensity of a superposition of two coherent harmonic waves of intensities  $I_1$  and  $I_2$ , and phase difference  $\phi$  is:

$$I = I_1 + I_2 + 2\sqrt{I_1 I_2} \cos\phi$$

If  $r = \frac{E_2}{E_1}$  is the ratio of the fields, then  $\phi = \arg(r)$  and  $\frac{I_2}{I_1} = |r|^2$ .

$$I \propto 1 + |r|^2 + 2|r|\cos\phi$$



**ILL. 1.2** Interferogram from Michelson interferometer with CW laser and swept reference arm

$$i(\tau_m) \propto 1 + |r|^2 + 2|r|\cos[\omega(\tau_m - \tau_o) + \phi_r]$$

This periodic function of the delay time difference  $\tau = \tau_m - \tau_o$  is called an interferogram. Since the interferogram is recorded by moving the mirror, it is often expressed in terms of distances  $d_r = c\tau_m$ ,  $d_o = c\tau_o$ , and the difference  $d = d_r - d_o = c\tau$ .

The fringes of the interferogram have a visibility (ratio of the amplitude of the sinusoidal component to the background) equal to  $\frac{2|r|}{(1 + |r|^2)}$ . This may be used to determine the reflectance  $\mathfrak{R} = |r|^2$  of

the object. If  $r$  is known to be real, i.e.,  $\phi_r = 0$ , then the depth of the object  $d_o$  may be estimated by noting that the interferogram has a maximum value when  $\tau = 0$ , i.e., when  $\tau_o = \tau_m$  or  $d_o = d_r$ .

However, since there are many maxima separated by the period  $\frac{2\pi}{\omega}$ , which corresponds to a distance  $c\left(\frac{2\pi}{\omega}\right) = \lambda$ , there is an ambiguity in the estimation of the depth equal to an integer multiple of the wavelength. This poses a principle difficulty, known as the phase wrap problem.

### Example 1.1

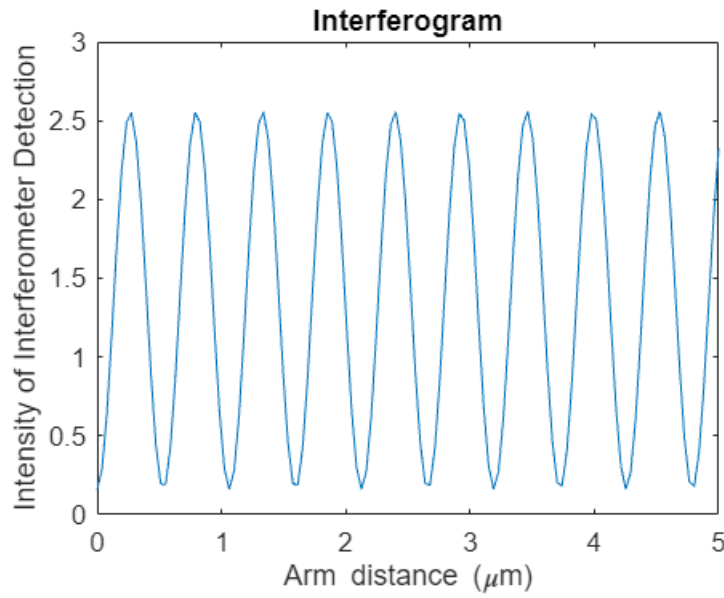
Interferogram from CW laser

```
% michelson interferometer for single surface CW wave
lambda0 = 0.532; % wavelength unit um
z_step = lambda0/4;
z=0.266; % the distance of sample arm, unit mm
r=0.6;% relative reflectivity
phi_r = 0; % the phase of the reflector

% swept reference arm distance between 0 and 5 um
d = linspace(0,5,128); % the distance, unit um
% interferogram

intf = 1+r.^2+2*r.*cos(2*pi./lambda0.*(z-d)+phi_r);

figure()
plot(d,intf);
set(gcf,'Position', [100 100 400 300])
title('Interferogram')
xlabel('Arm distance (\um)')
ylabel('Intensity of Interferometer Detection')
```

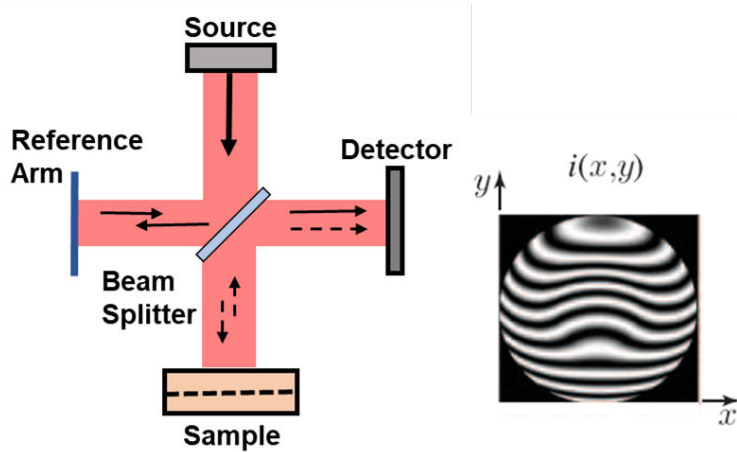


### 1.2.1 Depth topography

When the range (depth or elevation) of the surface of the object is position dependent, i.e.,  $d_o = d_o(x, y)$ , the measured intensity at a fixed position of the mirror (fixed  $d_r$ ) is an image

determined from (Eq.1) by substituting  $\tau = \frac{d}{c}$  and  $\omega = \frac{2\pi c}{\lambda}$ ,

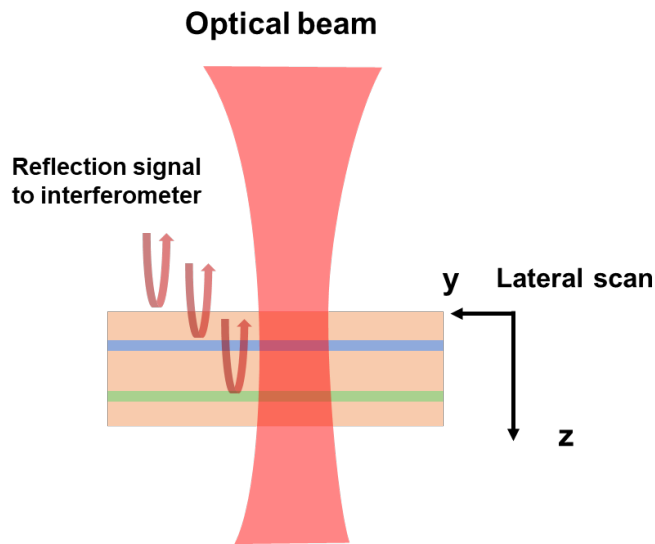
$$i(x, y) \propto 1 + |r|^2 + 2|r| \cos \left[ 2\pi \frac{d_r - d_o(x, y)}{\lambda} + \phi_r \right]$$



**ILL. 1.3** Interferogram  $I(x, y)$  recorded by a CCD camera in a Michelson interferometer used to image the topography of a surface of depth  $d_o(x, y)$ .

### 1.3 Limitations of single wavelength CW interferometry for axial imaging

Axial imaging takes the reflected signal (from all back scattering), interfering with the reference beam. The goal is to identify the scatterer location and reflectivity  $R(y, z)$  from the interferogram. The imaging along direction  $y$  is achieved through lateral scanning of the beam.



### ILL. 1.4 Axial imaging through interferometer

#### Example 1.2

Interferogram for axial imaging

```
% interferometer for single surface
z=linspace(0,5,128); % the distance, unit mm
y=linspace(1,50,32); % transverse direction, unit mm
[Y,Z]=ndgrid(y,z);
R=zeros(length(y),length(z));% relative reflectivity matrix

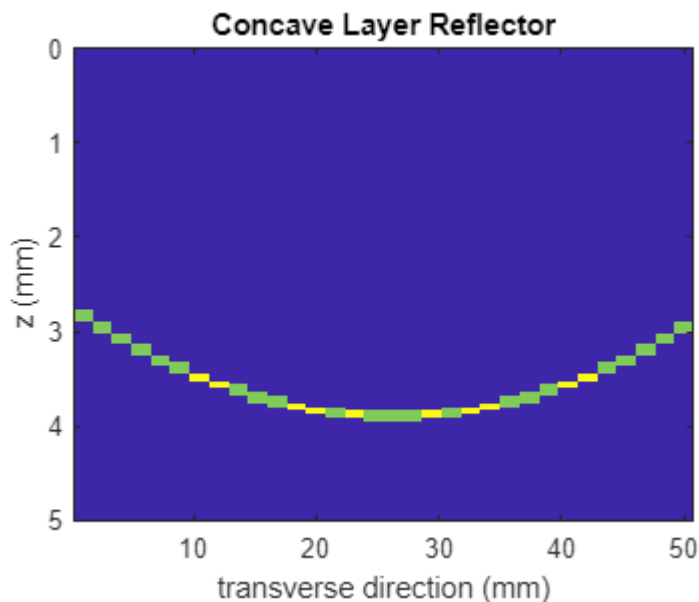
layer = "Concave Layer Reflector";

if strcmp(layer,'Single Layer Reflector')
    R(Z==z(50))=0.2;
elseif strcmp(layer,'Tilted Layer Reflector')
    R(ceil(20*Z-Y-20*z(10))==0)=0.2;
elseif strcmp(layer,'Concave Layer Reflector')
```

```

    radi=600;
    R(round( (radi*(Z-z(100)))+( Y-y(end/2) ).^2)/radi*10 )==0)=1;
    R_c= repmat(sum(R,2),[1,length(z)]); % normalization factor
    R=R./R_c*.1;
elseif strcmp(layer,'Double Layer Reflector')
    R(Z==z(30))=0.2;
    R(Z==z(50))=0.1;
end
R_90 = rot90(R,3);
figure()
imagesc(y,z,R_90)
set(gcf,'Position', [100 100 400 300])
title(layer)
xlabel('transverse direction (mm)')
ylabel('z (mm)')

```



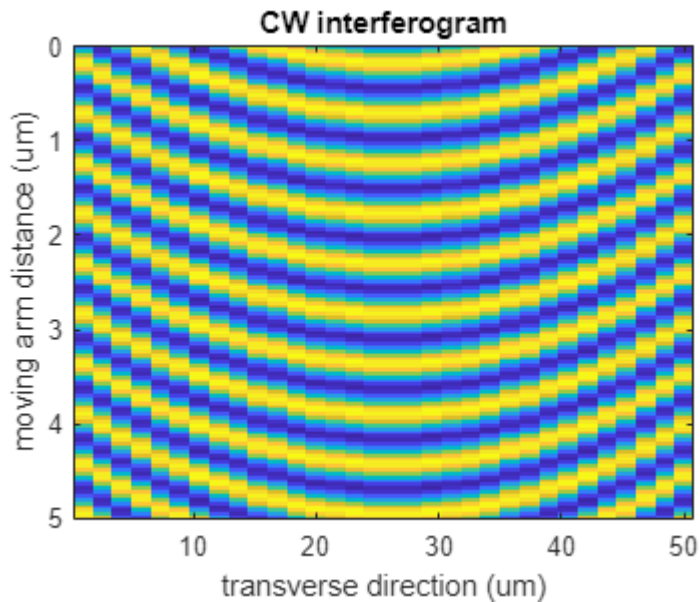
```

%% single wavelength generate interferogram
lambda0 = 0.532; % unit um
% swept arm distance
d = linspace(0,5,128); % the distance, unit um
% interferogram
Ing = zeros(length(y),length(d));

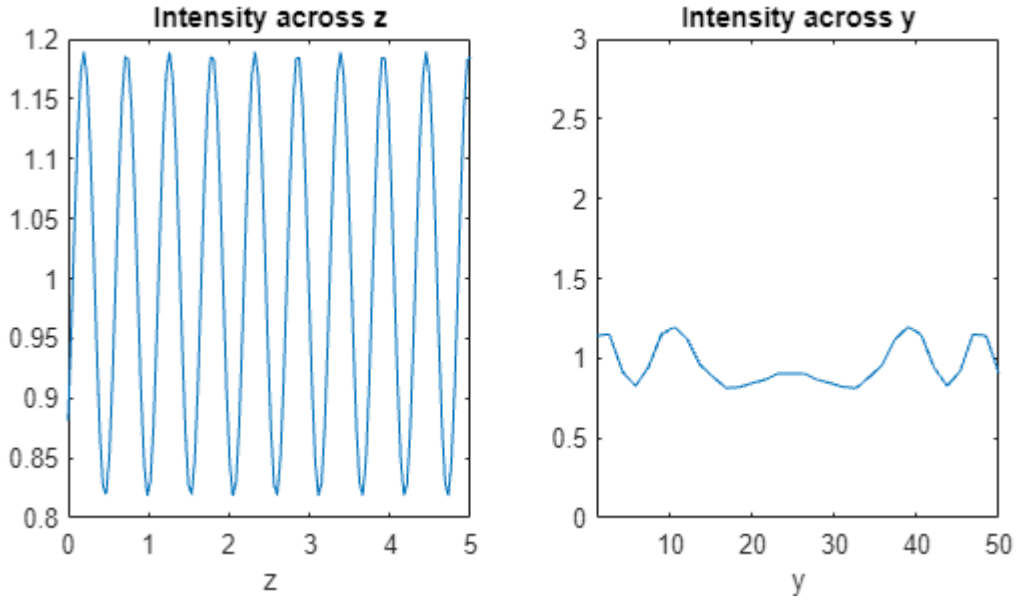
for ii=1:length(d)
    Ing(:,ii) = 1+sum(R.^2+2.*R.*cos(2*pi./lambda0.*(Z-d(ii))),2);
end
Ing_90 = rot90(Ing,3);

```

```
figure()
imagesc(y,d,Ing_90);
set(gcf,'Position', [100 100 400 300])
title('CW interferogram')
ylabel('moving arm distance (um)')
xlabel('transverse direction (um)')
```



```
figure()
set(gcf,'Position', [100 100 600 300])
subplot(121) %Intensity across z slice
plot(d,Ing(5,:));
title('Intensity across z')
xlabel('z')
xlim([0,5]);
subplot(122)%Intensity across y slice
plot(y,Ing(:,10)); axis([y(1),y(end),0,3])
title('Intensity across y')
xlabel('y')
```



### Can the CW interferogram be used for depth imaging?

While the interferogram in ILL. 1.3 provides some information on the reflectance and the distance  $d_o = c\tau_o$  to a single reflector, it cannot be used to simultaneously locate multiple reflectors at different depths within an object, i.e., it cannot be used for axial imaging (estimation of the reflectance  $r$  as a function of the depth  $z$ ). Suppose, for example, that the object has two reflectors with amplitude reflectance  $r_1$  and  $r_2$  at depths  $d_1$  and  $d_2$ , corresponding to time delays  $\tau_1$  and  $\tau_2$ . In this case, the interferogram

$$i(\tau_m) \propto 1 + \mathfrak{R}_b + 2|r_1|\cos[\omega(\tau_m - \tau_1) + \phi_1] + 2|r_2|\cos[\omega(\tau_m - \tau_2) + \phi_2],$$

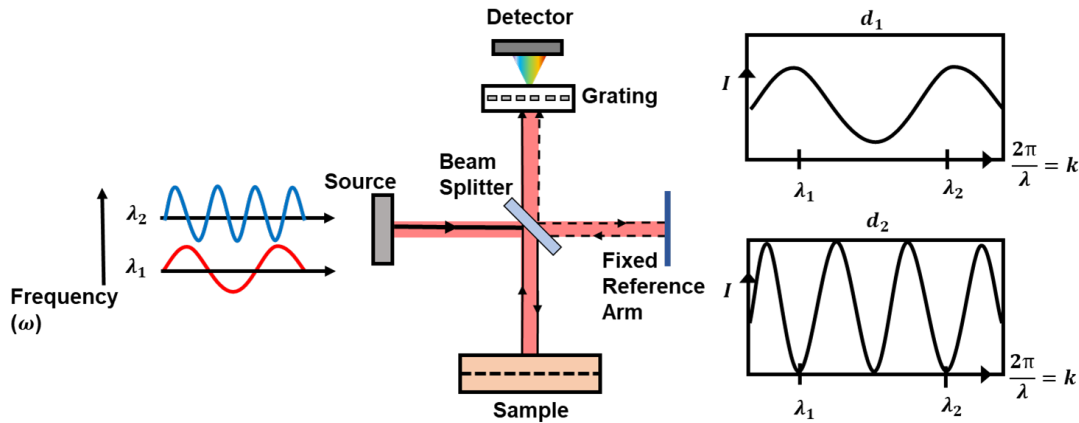
has two sinusoidal terms of the same angular frequency  $\omega$  but different amplitudes and phases ( $\mathfrak{R}_b$  is a constant background, and  $\phi_1$  and  $\phi_2$  are the phases associated with  $r_1$  and  $r_2$ ). Since the sum of the sinusoidal terms is equal to a single sinusoidal function of  $\tau_m$  with frequency  $\omega$  and an amplitude and a phase related to the amplitudes and phases of the two components, it is not possible to uniquely separate the two amplitudes and two phases (four unknowns and two equations) to provide estimates for the reflectance and depths of the two reflectors.

## 2. Interferometry with a swept frequency CW source



$$i(\tau_m, \omega) \propto 1 + R_b + \sum_{\ell} 2|r_{\ell}|\cos[\omega(\tau_m - \tau_{\ell}) + \phi_{\ell}]$$

Measure  $i(\tau_m, \omega)$  at a set of frequencies,  $\omega$ , and solve the inverse Fourier transform problem for  $|r_{\ell}|$  and  $\tau_{\ell}$ .



ILL. 2.1 Interferometry with a swept frequency CW source

### Example 2.1

Interferometry with a swept frequency CW source

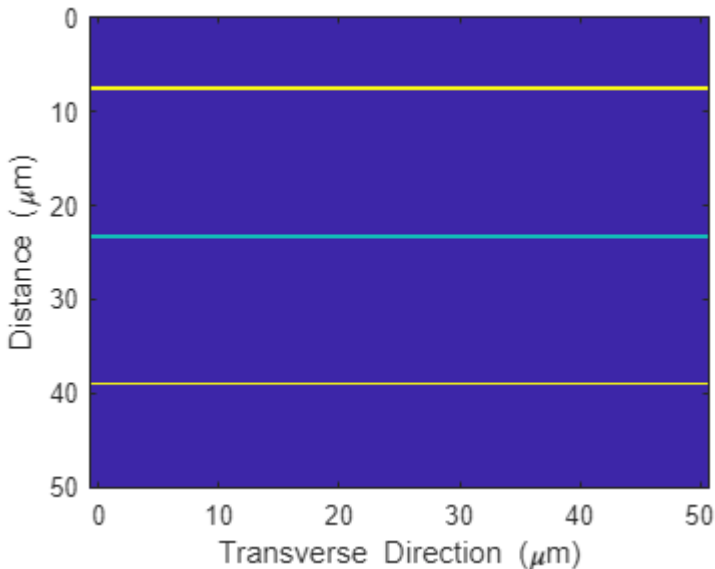
```
% interferometer for single surface
lamda0 = 0.7; % starting wavelength[unit: um]
lamda1 = 1.3; % end wavelength[unit: um]
k= 2*pi*linspace(1/lamda0,1/lamda1,128); % sweeping wavelength
% (k is wave number unit um^-1)
z=linspace(0,50,128); % the distance, unit um
y=linspace(0,50,32); % transverse direction, unit um
[Y,Z]=ndgrid(y,z);
R=zeros(length(y),length(z));% relative reflectivity matrix

layer = "Multiple Layer Reflector";
if strcmp(layer,'Single Layer Reflector')
    R(Z==z(20))=0.2;
elseif strcmp(layer,'Multiple Layer Reflector')
    R(Z==z(20))=0.2;
    R(Z==z(60))=0.1;
    R(Z==z(100))=0.2;
end
```

```

R_90 = rot90(R,3);
figure()
imagesc(z,y,R_90)
set(gcf,'Position', [100 100 400 300])
ylabel("Distance (\mu m)")
xlabel("Transverse Direction (\mu m)")

```

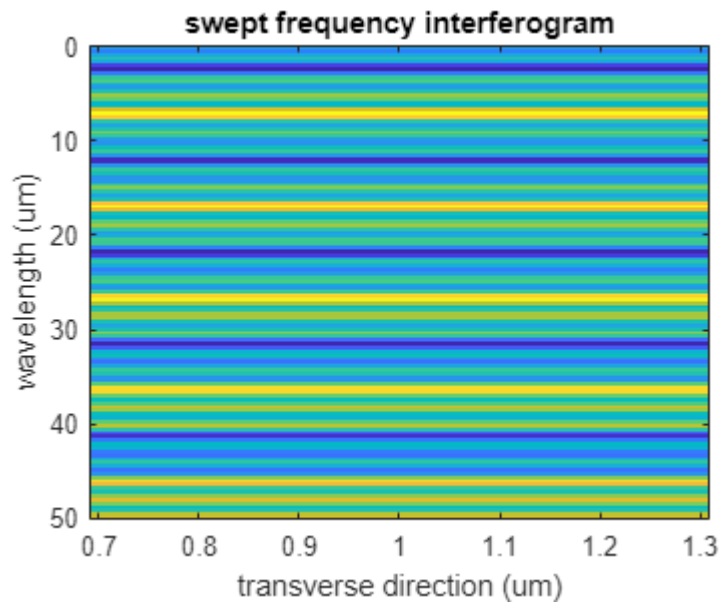


```

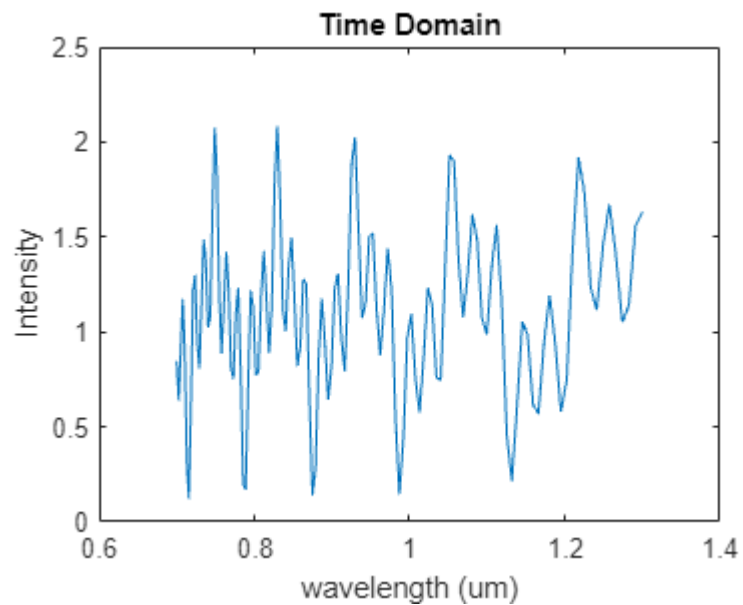
%% swept frequency interferogram
% reference arm distance
d = 0; % the distance of one arm, unit um
% interferogram
Ing = zeros(length(y),length(k));

for ii=1:length(k)
    Ing(:,ii) = 1+sum(R.^2+2*R.*cos(k(ii).*(Z-d)),2);
end
Ing_90 = rot90(Ing,3);
figure()
set(gcf,'Position', [100 100 400 300])
imagesc(2*pi./k,y,Ing_90);
title('swept frequency interferogram')
ylabel('wavelength (um)')
xlabel('transverse direction (um)')

```



```
figure()
set(gcf, 'Position', [100 100 400 300])
plot(2*pi./k, Ing(5,:));
%plot(k, Ing(5,:));
title('Time Domain')
xlabel('wavelength (um)')
ylabel('Intensity')
```

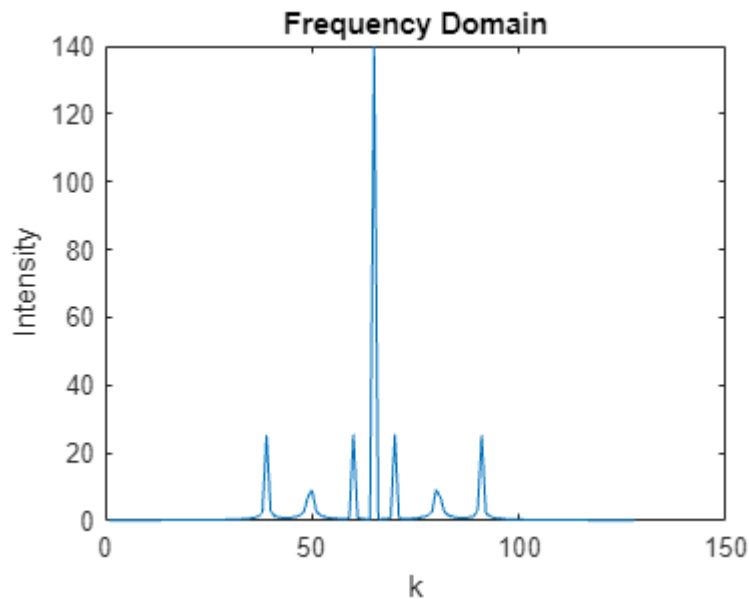


```
%% frequency domain OCT
```

```

a=fftshift(fft(Ing(5,:)));
figure()
set(gcf,'Position', [100 100 400 300])
plot(abs(a))
title('Frequency Domain')
xlabel('k')
ylabel('Intensity')

```



By sweeping the frequency, the interferogram is a function of  $\omega$ , instead of  $\tau$  (or  $d$ ). Example 2.1 shows a similar type of 2D object. The depth information ( $z$ ) is encoded in frequency.

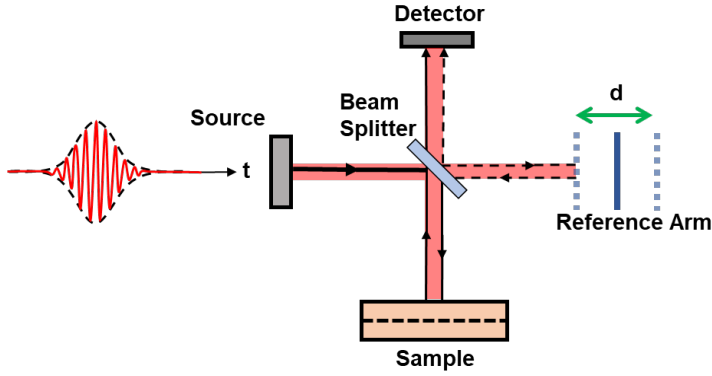
The depth information reconstruction can be done through inverse Fourier transform.

### 3. Interferometry with low coherent source

#### 3.1 Interferometry with pulsed wave

An ultrashort pulse may be directly used for axial imaging using flight measurements. The detector must be sufficiently fast to determine the time of arrival with high resolution.

An ultrashort pulse may be used with a slow detector in an interferometric configuration.



### ILL. 3.1 Interferometry with pulsed light

The total intensity is proportional to  $|U(t - \tau_m) + rU(t - \tau_o)|^2$ . If the detector is slow in comparison with the pulse width, it simply measures the area under the intensity function. This is the same as the area under the function  $|U(t) + rU(t + \tau)|^2$ , where  $\tau = \tau_m - \tau_o$ . Integrating the four terms in the sum

$$|U(t) + U(t + \tau)|^2 = |U(t)|^2 + |r|^2|U(t + \tau)|^2 + rU^*(t)U(t + \tau) + r^*U(t)U^*(t + \tau)$$

leads to the following expression for the measured signal:

$$i(\tau) = (1 + |r|^2)G(0) + 2\text{Re}\{rG(\tau)\} = G(0) [1 + |r|^2 + \text{Re}\{rg(\tau)\}]$$

where

$$G(\tau) = \int_{-\infty}^{\infty} U^*(t)U(t + \tau) dt$$

is the autocorrelation function of the pulse envelope,  $G(0)$  is the area under the pulse intensity, and  $g(\tau) = G(\tau)/G(0)$ .

$$U(t) = A(t)\exp(j\omega_0 t)$$

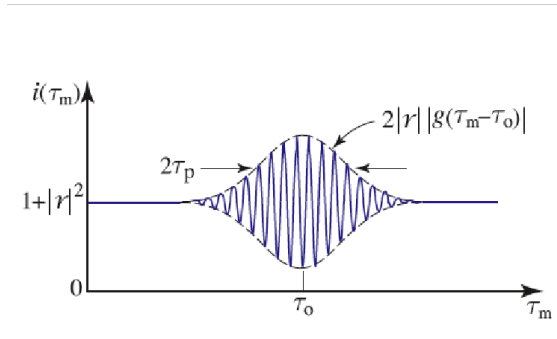
$$G(\tau) = G_A(\tau)\exp(j\omega_0 \tau)$$

$$g(\tau) = |g_A(\tau)|\exp[j(\omega_0 \tau) + \phi_A]$$

$$\phi_A = \arg\{G_A(\tau)\}, \text{ where } \tau = \tau_m - \tau_o$$

Pulsed-Wave Interferogram:

$$i(\tau_m) \propto 1 + |r|^2 + 2|r||g(\tau_m - \tau_o)|\cos[\omega_0(\tau_m - \tau_o) + \phi], \text{ where } \phi = \phi_A + \arg\{r\}$$



### ILL. 3.2 Interferogram of a pulsed wave

The pulsed-wave interferogram extends over an interval equal to twice the pulse width.

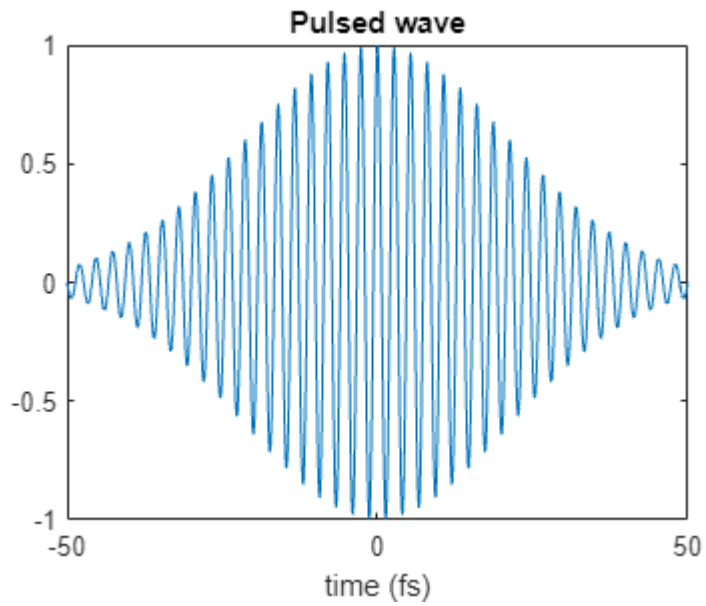
#### Example 3.1

Pulsed-wave interferogram

```
% pulsed wave
% a gaussian shape pulse with width 10 fs. central wavelength 800 nm.
lambda0=0.8; %central wavelength, unit um.
c=3e8; %speed of light m/s
omega0=2*pi*c/(lambda0*1e-6);

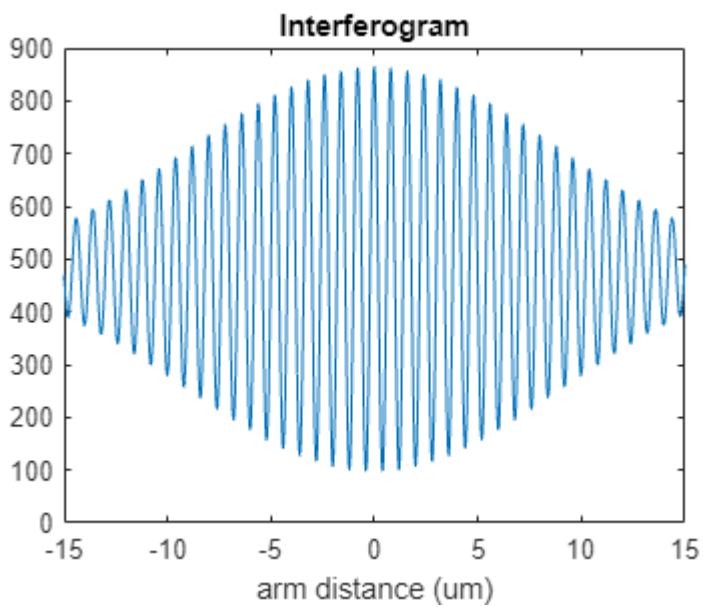
t=linspace(-50,50,1024); % unit fs
r=0.5; %reflectivity
tau = 30; % pulse duration [unit: fs] Please make this a slide bar from
10:10:50.
a = exp(-t.^2./tau^2); %pulse envelope with pulse width ~ 20 fs

u = a.*exp(1i.*omega0.*t*1e-15);
g0 = sum(u.*conj(u));% total pulse power
g_tau = conv(u,u,'same')/g0;
figure()
plot(t,real(u))
set(gcf,'Position', [100 100 400 300])
xlabel('time (fs)')
title('Pulsed wave')
```

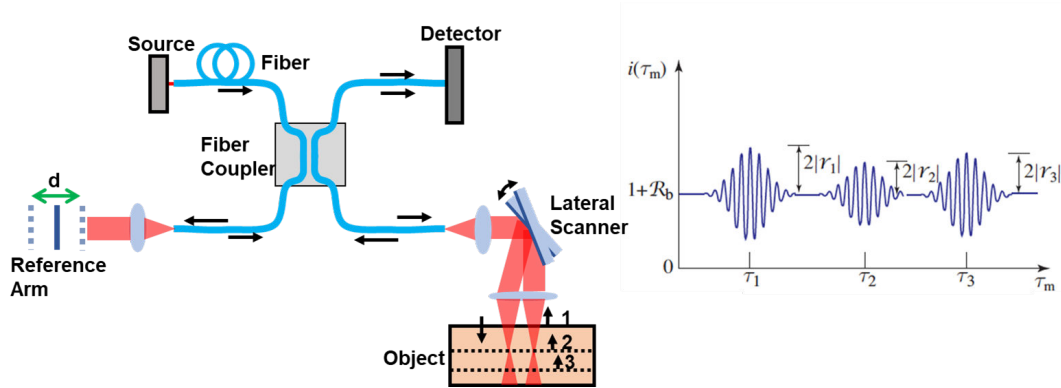


```
%%
inf=g0*(1+r^2+2*real(r*g_tau));

figure()
plot(3e8.*t.*1e-15*1e6,inf);
set(gcf,'Position', [100 100 400 300])
xlabel('arm distance (um)')
title('Interferogram')
```



### 3.2 Time domain Optical Coherent Tomography (OTC)



ILL. 3.3 Time Domain Optical Coherent Tomography (TD-OCT) using low coherent source

$$i(\tau_m) \propto 1 + |r|^2 + 2|r||g(\tau_m - \tau_0)|\cos[\omega_0(\tau_m - \tau_0) + \phi]$$

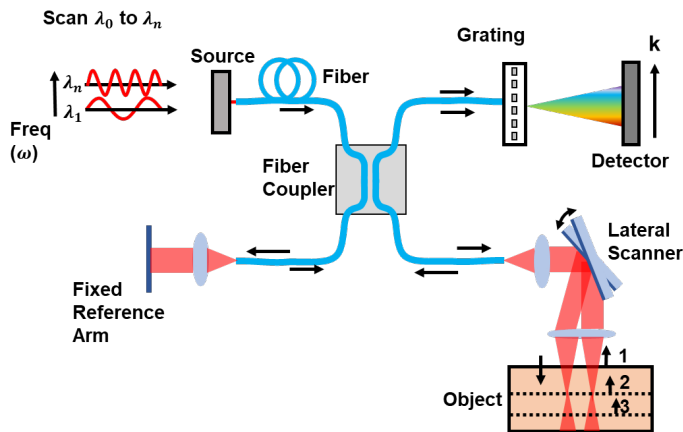
Coherence function:

$$G(\tau) = \langle U^*(t)U(t + \tau) \rangle$$

Complex degree of coherence:

$$g(\tau) = \frac{G(\tau)}{G(0)}$$

#### 3.2.1 Comparison of TD- vs. FD-OCT



ILL. 3.4 Frequency domain OCT (FD-OCT), with a source scanned from  $\lambda_0$  to  $\lambda_n$  and a fixed reference arm.



**Sensitivity:** FD-OCT typically has a higher sensitivity compared to TD-OCT. This enables clearer images and better imaging of structures deeper within tissues.

**No Moving Parts:** As mentioned above, TD-OCT relies on a mechanically moving reference mirror to obtain depth scans, which can be a source of wear and tear and reduce system longevity. FD-OCT doesn't need a moving reference arm, leading to increased system durability.

**Speed:** Due to the slow movement of the reference arm in TD-OCT, FD-OCT systems can acquire data significantly faster, making it more suitable for imaging areas that move.

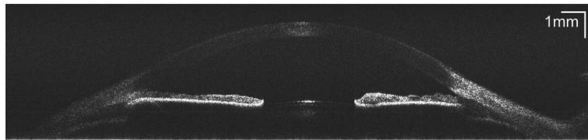


Fig. 6. Cross-sectional image of the anterior chamber together with cornea and anterior surface of crystalline lens acquired in *enhanced imaging range mode*.

**ILL. 3.5** *Anterior OCT of the cornea and lens, from Gora, Michalina, et al. "Ultra high-speed swept source OCT imaging of the anterior segment of human eye at 200 kHz with adjustable imaging range." Optics Express 17.17 (2009): 14880-14894.*